Improvement of Savonius wind turbine performance with using wind collector

B. Deda Altan[a,*] and A. Gungor[b]

[a,b] *Akdeniz University, Faculty of Engineering, Department of Mechanical Engineering, Antalya, 07058, Turkey.*

Abstract

In this study, the improvement of the turbine performance of Savonius, one of the vertical axis wind turbines, was carried out numerically. The numerical approach used in the improvement studies was supported by experimental results and was confirmed. Within the scope of this improvement, a wind collector was placed in the turbine front zone to decrease the negative moment on the counter-rotating blade of the Savonius turbine. To obtain the highest turbine performance, all of the changes in the design parameters of this wind collector, such as the wind inlet width, wind outlet width, collector length, and collector height, were examined, and ideal design parameters of the collector were specified. The geometric parameters of the investigated wind collector were taken depending on the circular dimension of the Savonius turbine used. Unsteady simulations for different geometric parameters using the sliding mesh approach were performed in the CFD program. According to the numerical analysis results, the power-coefficient of the conventional turbine was increased to 0.23 levels by using the wind collector with the ideal geometric parameters. Thus, with the use of a wind collector, the power coefficient of a conventional Savonius wind turbine was improved by about 54%.

Keywords: Wind, Savonius, Energy, Design, Wind collector

**** Corresponding author.***

E-mail address: bdeda@akdeniz.edu.tr (B. Deda Altan)

1. Introduction

The interest in renewable energy sources is increasing day by day due to the decrease in the reserves of fossil energy sources and the environmental problems they have created. One of these renewable energy sources is wind energy. In order to benefit from wind energy, horizontal and vertical axis wind turbines are used [1-5]. One of these vertical axis wind turbines is Savonius wind turbines. With their very simple construction, Savonius wind turbines are highly suitable turbines, especially for generating electricity in rural areas. In particular, their low running speeds, high starting torques, simple construction, and easy maintenance increase the demand for the use of these turbines. Savonius wind turbines were invented by Sigurd Savonius in the 1920s. These turbines basically have a simple structure formed by two symmetrically shifting semi-cylinders, which basically consist of concave and convex surfaces.

Considering the literature studies on this subject, is seen that many numerical and/or experimental studies on Savonius wind turbines have been carried out and are still being carried out. In a group of studies, various turbine structural parameters, such as the overlap ratio, separation ratio, blade type design and blade tip plate were investigated numerically and experimentally [6-10]. In another group of studies, various designs were made to provide turbine performance increase to the front zone of the Savonius turbine [11-15]. Mahmud et al. [16] investigated the effect of aspect ratio on the performance of a conventional turbine in their experimental study. Gad et al. [17] conducted analysis with modified design of conventional blades. Saad et al. [18] examined the effects of the overlap ratio on the efficiency of the Savonius turbine with a twist angle. Layeghmand et al. [19] designed a new deflector system by numerical method to improve the efficiency of the rotor. They improved the coefficient of power of the Savonius rotor by 32% compared to its conventional version. Yahya et al. [20] examined the effect of the guide vanes they designed on the performances of the rotor. They found that the power coefficient increased by around 68%. Mohamed et al. [21] designed an obstacle shielding plate. In this direction, they declared that they increased the power-coefficient of the two-bladed Savonius rotor by about 52%. Tartuferia et al. [22] increased the power-coefficient of the two-bladed classical SWT by about 20% using a conveyor-deflector curtain. Kalluvila et al. [23] examined the performance of the Savonius rotor with the guide blade system arranged around the Savonius rotor. Thus, they enhanced the power-coefficient of the Savonius by 55%. Nimvari et al. [24] increased the power-coefficient of a Savonius rotor by about 10% compared to the classical version by using a porous deflector. Hesami et al. [25] with their design called wind lens, they carried out investigations on various Savonius wind turbine configurations. They found the effect of the wind lens on the single- and two-bladed Savonius turbine as an increase in the power-coefficient of about 26% compared to its classical form. When other relevant literatures were examined, the power-coefficient of the turbine was improved threefold compared to its non-apparatus state by using the wind router apparatus without any modification in the classical Savonius turbine [26]. With a passive deflector that can be self-directed according to the wind direction, the performance of the conventional Savonius turbine was increased by an average

of 25% [27]. By investigating the effects of flat plate on turbine efficiency in case of dual use of SWTs, the power coefficient of the turbine was increased by about 42% [28]. With the change in the shape of the truncated cone axisymmetric deflector placed on the end plates of the SWT, the turbine performance was improved by an average of 20% compared to the linear surface of the truncated cone deflector [29]. With the optimum Savonius turbine geometric parameters obtained by using artificial neural networks, the maximum C_p value was increased to about 66% [30].

In this study, a wind collector was designed in front of the turbine to eliminate the torque acting on the Savonius turbine in the opposite direction and to increase the wind speed entering the turbine in order to improve the performance values of Savonius wind turbines such as power and torque coefficients. With this design, the optimal dimensions of all design parameters of the wind collector such as wind inlet width, wind outlet width, collector height and collector length were determined in order to obtain the best performance values.

2. Design and method

The Savonius-type wind turbine (SWT) is a VAWT that has certain advantages, such as its simple structure, low cost, and high starting torque. Despite these advantages, these turbines are less used than Darrieus turbines, which are another type of VAWTs with higher turbine performance data when compared to Savonius turbines. Generally, Savonius turbines are equipped with two blades; one is convex and the other is concave. As the turbine starts to rotate, the concave blade produces positive torque and the convex blade produces negative torque. This negative torque reduces the turbine performance. This low performance should be improved to increase the use of SWTs. Improving the performance of SWTs is possible with different types of blade designs and hybrid turbine systems, as well as by preventing the formation of negative torque. Here, a wind collector design was installed on the side of the turbine that meets the wind to improve the turbine efficiency. Thus, this wind collector prevented the negative torque and also controlled the upstream wind velocity. The wind collector placed anteriorly to the turbine is shown in Figure 1. With this additional wind collector, designed to be placed anteriorly to the turbine, without modification of the turbine structure, the performance of the turbine was analyzed. The designed wind collector consisted of an equal-angle part and an open-outlet channel.

The geometric dimensions of the SWT analyzed are shown in Figure 2. The geometric dimensions of the turbine, which were determined at the beginning, were kept constant throughout this study. The design parameters of the SWT were taken as the diameter D = 2R = 46 cm, blade tip plate diameter D_0 = 1.1D, height H = 46 cm and ratio of the overlap e/d = 0.15.

Different geometric dimensions of the wind collector, shown in Figure 3, were examined to determine the effects of the wind collector on the SWT performance. The design parameters of the wind collector; b: collector outlet width, a: collector inlet width, c: collector length, g: collector position, h: collector height, and n: collector outlet channel length. The

dimensions of the wind collector were designed depending on the dimension of the turbine. According to this; the ratio of collector outlet width to the radius of the turbine (b/R), the ratio of the collector inlet width to the radius of the turbine (a/R), the ratio of the collector length to the radius of the turbine (c/R), the ratio of the collector position to the radius of the turbine (g/R), and the ratio of the collector height to the diameter of the turbine (h/2R). Throughout the study, the length of collector outlet channel (n) was taken as the same as the length of collector position (g). According to the design of the collector, the outlet channel width of the collector was taken as the same as the collector outlet width.

As given in Table 1, (b/R) ratio between 0.8 and 1.4, (a/R) ratio between 4 and 7, (c/R) ratio between 1 and 3, (g/R) ratio between 1.15 and 1.4 and the (h/2R) ratio was changed between 1.2 and 1.6. Thus, the effects of the design ratios of the wind collector were examined.

Here, a dynamic analysis was performed with the ANSYS Fluent to determine the effects of an additional design such as a wind collector on the turbine torque and power coefficients. The wind speed used in dynamic analyses was taken as 8 m/s. Figure 4 shows the computational domains and boundary conditions used in numerical simulations. The computational domain dimensions were formed depend on the turbine diameter. The computational domains were formed in two parts as rotating domain and steady domain. The rotating flow domain was designed to contain the Savonius turbine model and the steady flow domain was designed to contain the wind collector. An interface was formed for the continuity of the flow outside and inside the turbine. The dimensions of the flow domain were chosen according to the turbine diameter, where turbine performances were not affected. The inlet boundary was placed 8D upstream of the turbine. The outlet boundary was placed 8D downstream of the turbine.

The performance analyses were carried out with the results of this numerical study. The performance coefficients of the SWT were found using the power and torque equations. The equations of torque and power coefficients are given in Eq. (1) and Eq. (2), respectively. Also, the tip speed ratio is given in Eq. (3).

$$C_t = \frac{T_{pr}}{T_w} = \frac{T_{pr}}{\frac{1}{2}\rho A V^2 R} \tag{1}$$

$$C_p = \frac{P_{pr}}{P_w} = \frac{P_{pr}}{\frac{1}{2}\rho A V^3} \tag{2}$$

$$\lambda = \frac{\omega R}{V} \tag{3}$$

The starting position of the turbine for the first movement was chosen to be perpendicular to each other with the wind direction coming to its blades. First of all, in order to ensure the

validation of the numerical solution, the mesh independence study was conducted by considering the average coefficient of torque at the constant TSR. The number of first mesh elements, where these average torque coefficients were always the same, was considered. Then by dividing a complete turbine revolution into time steps, the performance changes in each time step were obtained numerically. In order to determine that the incoming wind flow and the Savonius turbine rotation were in a stable regime, the analyses were continued until that the values obtained from the relevant time steps, as shown in Figure 5, were always the same. In order to better analyze the stability here, the turbine was made 6 full cycles. As seen from the figure, it was observed that the torque production was always the same after the third cycle of the turbine. It was observed that the coefficient of torque values found during the first one or two rotations of the turbine were variable due to the fact that the linear wind flow coming from the inlet section of the numerical flow domain coincided with the flow field rotating around the turbine. Later, it was also determined that the wind flow became stable as it continued to flow in this way. The time steps were taken into account from the fourth rotation so that the analysis results could always be determined under the same stable conditions.

The study of time independence of time steps is shown in Figure 6. In this analysis, the torque coefficient obtained by numerical analysis was performed to be almost the same as the experimental torque coefficient [13] value determined at a constant TSR of 0.6.

Here, one rotation of the SWT was sliced by angles of 7.5°, 5° and 2.5° degrees. With these divided angle slices, 48-, 72- and 144-time steps were formed, respectively, in one full rotation of the turbine. The turbine performance data in a full turbine rotation were obtained over these time steps. Thus, the variation of the coefficients obtained at a stable full turbine rotation is shown in the figure. It was found that these variations were almost the same, but differed in the angle of rotation of 135° degrees and 315° degrees. The time step independence was found by comparing the averaged numerical torque coefficients with the experimental torque coefficient. When evaluated in this respect, it was found that the average coefficient of torque obtained with 72-time steps was almost the same as the value obtained with 144-time steps, and there was more difference between them and the value obtained with 48-time steps. Because the results were almost the same in the time step after 72-time steps, and especially because of the long analysis time, the results obtained with this time step were taken into account. Thus, time periods in which the numerical results of the time steps almost do not change over time were obtained.

In Figure 7, the change of the power-coefficient according to the TSR is shown both experimentally [13] and numerically. The power coefficients were determined according to the coefficients of torque obtained from the numerical analysis at different TSRs. As seen in Figure 7, the variations in numerical and experimental coefficients of power supported each other harmoniously. Therefore, the numerical solution methodology used in the study was confirmed by the literature experiment results.

Figure 8 presents a meshed section of the numerical system used throughout the study. The numerical system consisted of two domains: steady and rotating. These two domains were separately meshed with the tetrahedrons type unstructured meshing method. The same mesh

of numerical data was used throughout the study. Thus, the best parameters were obtained as a result of the comparison of the performance values obtained in a variety of geometric parameters. Analyzes were made using the standard k-ε turbulence model. The y+ dimensionless value was set above 30. The solutions were made using the secondary interpolation method. SIMPLE algorithm was utilized for pressure-velocity distribution.

3. Results and discussion

This study investigated the effects of the changes in a variety of geometric parameters of the designed wind collector on the SWT performances. As performances, the torque and power coefficients obtained during a cycle of the turbine were considered. In order to compare these coefficients obtained throughout the study, the fixed TSR was taken as 0.6. Thus, the effect of the geometrical parameters of the wind collector was investigated. Figure 9 shows the effects of the changes in the ratio of the outlet width of the wind collector (b/R) under the fixed TSR on the coefficient of torque, based on the values of 0.8, 1, 1.1, 1.2, 1.3, and 1.4. Other geometric parameter ratios, such as a/R = 4, c/R = 2, g/R = 1.2, and h/2R = 1.4, were taken as constants values, in order to analyze the effect of the collector outlet width only. In order to understand the effect of the use of collector on turbine performance, the performance results of the turbine without collector were also determined. As seen in Figure 9, it was found that the turbine torque coefficients with wind collector were higher than the turbine without collector. The formation of a negative torque coefficient was found to be more as a result of that the output width was narrower than other widths only with the presence of the b/R ratio of 0.8. In this case, it negatively affected the average turbine coefficient of torque. To obtain the average coefficient of torque as the maximum value, the cases where negative values did not occur during a complete rotation of the turbine, and where the positive values appeared to be at their maximum values were considered. Accordingly, the b/R ratio value, at which the maximum changes were obtained, was 1.1. As shown in Figure 9, the maximum C_t of the turbine equipped with the collector at this ratio value was higher than the angle range, at which the maximum coefficients of torque of the turbine without collector were obtained. By using a wind collector, the wind was directed to the concave blade and the effect of the convex blade producing negative torque was tried to be minimized. Thus, maximum positive torque coefficients were obtained in the wider-angle range. Hence, it was ascertained that at different geometric ratios of the collector, the negative torque coefficient affecting the torque coefficient of the turbine was decreased or eliminated.

Figure 10 shows the velocity contours of various b/R ratios. In all analyses, the value of TSR was taken as 0.6. When Figure 10 was examined, it was observed that the flow escaped mostly from the closed side of the channel at b/R ratios values of 0.8 and 1. When the b/R ratio was 1.1, it was understood that the turbine blade fully met the incoming wind. Therefore, the greatest torque production was achieved at this ratio. It was observed that at values of the b/R ratio of 1.2 and above, the flow tried to escape from the open part of the channel. In this

case, it was found that the wind exerted a torque effect on the rotating convex blade in the opposite direction.

Figure 11 shows the effect of the different ratio of inlet width (a/R) on the torque-coefficient according to the rotation angle, with the presence of the determined b/R ratio of 1.1. In this regard, the a/R ratios were taken as 4, 5, 6, and 7. In order to determine the collector inlet width (a), the values of c/R = 2, g/R = 1.2, and h/2R = 1.4 were taken as constant values. In Figure 11, only the effect of collector inlet width was analyzed while keeping all collector design parameters constant. As can be seen in Figure 11, it was found that quite high torque-coefficients were obtained with the presence of an a/R ratio value of 5 and higher. And at these values, torque coefficients of approximately the same values were obtained. At an a/R value of 4, characteristically, the same torque coefficient was obtained, but a lower torque coefficient was obtained at other a/R ratios. It was ascertained from Figure 11 that maximum positive torque-coefficients found from the SWT equipped with a collector were in a larger range of turbine rotation angle when compared to the positive torque-coefficients found from the SWT without a collector. Especially when the turbine was examined according to the area swept during rotation; It was found that the area where the maximum positive torque-coefficients of the SWT with collector were obtained was 0.26 higher than the area where the maximum positive torque-coefficients of the SWT without collector were obtained. Therefore, it revealed that the use of collectors was of great importance for the improvement of the turbine performance.

Figure 12 shows variations in the torque coefficients found during the 0°–360° rotation of the turbine at different ratios of the wind collector length (c/R). The collector length c/R ratios were taken as 1, 2, and 3. Since the value of the outlet width ratio (b/R) of the wind collector was previously reported to be 1.1, while the value of the inlet width ratio of (a/R) was 5, these values were taken without change. In order to examine the effect of the collector length only, g/R = 1.2 and h/2R = 1.4 were taken as constants. As can be seen in Figure 12, it was ascertained that when the c/R ratios were 1 and 3, almost the same maximum and minimum torque coefficients were obtained. Accordingly, the best torque coefficient change was obtained from the situation where the c/R ratio value was 2. When the c/R ratio was 1 and 3, the flow separations were observed on the side inclined plates of the collector, and the torque coefficients were low because of this situation.

Figure 13 shows the results of the numerical analysis of the wind collector location ratio (g/R) at values between 1.15 and 1.4. According to this analysis, similar changes were obtained with g/R ratios of 1.15, 1.2, and 1.25, while lower changes were obtained at a ratio of 1.4. From previous numerical analyses, b/R = 1.1 was determined as a/R = 5 and c/R = 2. In this analysis, h/2R = 1.4 was taken as constant in order to reveal the effect of the location parameter. In the analysis performed on the g/R ratio, such as 1.4, some torque coefficient values of the turbine were found to be negative.

Figure 14 shows the effects of the design ratios of the collector on the average-torque coefficient. The average torque performance values obtained at different geometric ratios of the wind collector were compared both among themselves and with the values obtained from the turbine without collector. As a result of the comparison, the optimum geometric ratios of

the wind collector were determined. Average torque coefficient value of around 0.24 was obtained from turbine without wind collector. The maximum torque coefficient was found when the b/R ratio was 1.1. Since the coefficient of torque did not change significantly when the a/R ratio was 6 or 7, the a/R ratio value was chosen as 5 for ease of design and economy. As can be seen from the figure, the average coefficient of torque was obtained with the c/R ratio value of 2. The maximum average coefficient of torque was obtained at 1.2 value of g/R ratio as seen in the figure. In addition, as can be seen from the figure, it was found that the h/2R ratio, where the best average torque coefficient was obtained, was 1.4. Thus, the direction of the wind coming to the SWT was optimized by changing the parameters of the wind collector. Therefore, the optimal geometric ratios were determined as b/R=1.1, a/R=5, c/R=2, g/R=1.2 and h/2R=1.4.

Figure 15 presents the changes in the coefficient of power depending on the TSR, for a SWT both with and without a wind collector. In this regard, a wind collector with the geometric parameters of b/R = 1.1, a/R = 5 c/R = 2, g/R = 1.2, and h/2R = 1.4, according to the results of the numerical analysis, was used. It was found that the maximum coefficient of power for SWT with and without a collector was around 0.6 of the TSR. The use of a wind collector caused the wind speed to increase slightly and the wind to come only on the blade rotating in the downwind direction. Therefore, at the same time, it was determined that the use of a wind collector also caused a slight increase in the TSR. It was determined that the maximum C_p of the turbine with collector is approximately 54% higher than the turbine without collector.

The change of the torque-coefficients of the turbines with and without wind collector is shown in Figure 16. It was found that the variations in the C_p of the turbine without a wind collector were in smaller values. As can be seen in Figure 16, the turbine angle segments, where the positive torque-coefficients were observed, increased as a result of the use of the wind collector; thus, increased turbine performance values were ensured.

4. Conclusions

In this study, a wind collector was placed in front of the turbine to improve the Savonius wind turbine performance. By changing the design parameters of this collector, it was tried to determine the design values at which the highest turbine performance was obtained. According to this, the effect of wind collector inlet width, outlet width, collector height, collector length and collector position on turbine were investigated. First of all, numerical analysis solution method was confirmed with experimental data in the literature.

According to the parameter studies, the optimal collector outlet width (b/R) ratio was determined as 1.1, collector inlet width (a/R) ratio was 5, collector length ratio (c/R) was 2, collector position ratio (g/R) was 1.2, and collector height ratio (h/2R) was 1.4. The turbine power coefficient value, which was 0.15 with a turbine without a collector, was increased to about 0.23 with a turbine with a collector in these optimal geometric parameters.

As a result, by using a wind collector, coefficient of power of the SWT was increased by about 54% from the coefficient of power of the turbine without a wind collector. Thus, it was found that the turbine performance was significantly improved by using the wind collector.

Nomenclature

a	Collector inlet width
b	Collector outlet width
c	Collector length
d	Blade diameter
e	Blade overlap distance
g	Collector position
h	Collector height
n	Collector outlet channel length
A	Swept area
CFD	Computational Fluid Dynamics
C_p	Coefficient of power
C_t	Coefficient of torque
D	Turbine diameter
D_0	Blade tip plate diameter
H	Turbine height
P_{pr}	Power of turbine
P_w	Power of wind
R	Turbine radius
SWT	Savonius Wind Turbine
T_{pr}	Torque produced by turbine
T_w	Torque generated by wind
TSR	Tip Speed Ratio
V	Wind speed
VAWT	Vertical Axis Wind Turbine
λ	Tip speed ratio
ρ	Density
ω	Angular velocity

References

1. Soltani, M.R., Birjandi, A.H., and Seddighi Moorani, M. “Effect of surface contamination on the performance of a section of a wind turbine blade”, *Scientia Iranica B*, **18**(3), pp. 349-357 (2011).

2. Roga, S. and Kumar Dubey, S. “DMST Approach for analysis of 2 and 3 bladed type Darrieus vertical axis wind turbine”, *EAI Endorsed Transactions on Energy Web,* **8**(33), pp. 1-33 (2020).

3. Maftouni, N. and Taghaddosi, M. "A CFD study of a flanged shrouded wind turbine: Effects of different flange surface types on output power", *Scientia Iranica B*, **29**(1), pp. 101-108 (2022).

4. Roga, S., Kisku, V., and Datta, S. "Performance of a vertical wind turbine with permanent magnet synchronous generator", *Proceedings of the Institution of Civil Engineers-Energy*, **175**(4), pp. 205-215 (2022).

5. Roga, S. "Wind energy investigation of straight-bladed vertical axis wind turbine using computational analysis", *EAI Endorsed Transactions on Energy Web*, **8**(33), pp. 1-9 (2020).

6. Alom, N. and Saha, U.K. "Performance evaluation of vent-augmented elliptical-bladed Savonius rotors by numerical simulation and wind tunnel experiments", *Energy*, **152**, pp. 277-290 (2018).

7. Akwa, J., Junior, G., and Petry, A. "Discussion on the verification of the overlap ratio influence on performance coefficients of a Savonius wind rotor using computational fluid Dynamics", *Renewable Energy*, **38**, pp. 141-149 (2012).

8. Deda Altan, B., Kovan, V., and Altan, G. "Numerical and experimental analysis of a 3D printed Savonius rotor with built-in extension plate", *Wind and Structures*, **27**(1), pp. 1-9 (2018).

9. Jeon, K.S., Jeong, J.I., Pan, J.K., et al. "Effects of end plates with various shapes and sizes on helical Savonius wind turbines", *Renewable Energy*, **79**, pp. 167-176 (2015).

10. Al-Ghriybah, M., Fadhli Zulkafli, M., Hissein Didane, D., et al. "The effect of spacing between inner blades on the performance of the Savonius wind turbine", *Sustainable Energy Technologies and Assessments*, **43**, 100988 (2021).

11. Goodarzi, M. and Keimanesh, R. "Numerical analysis on overall performance of Savonius turbines adjacent to a natural draft cooling tower", *Energy Conversion and Management*, **99**, pp. 41-49 (2015).

12. El-Askary, W.A., Nasef, M.H., Abdel-Hamid, A.A., et al. "Harvesting wind energy for improving performance of Savonius rotor", *Journal of Wind Engineering and Industrial Aerodynamics*, **139**, pp. 8-15 (2015).

13. Deda Altan, B. and Atılgan, M. "The use of a curtain design to increase the performance level of a Savonius wind rotors", *Renewable Energy*, **35**, pp. 821-829 (2010).

14. Manganhar, A.L., Rajpar, A.H., Luhur, M.R., et al. "Performance analysis of a Savonius vertical axis wind turbine integrated with wind accelerating and guiding rotor house", *Renewable Energy*, **136**, pp. 512-520 (2019).

15. Deda Altan, B. and Gungor A. "Examination of the Effect of Triangular Plate on the Performances of Reverse Rotating Dual Savonius Wind Turbines", *Processes*, **10**(11), 2278 (2022).

16. Mahmoud, N.H., El-Haroun, A.A., Wahba, E., et al. "An experimental study on improvement of Savonius rotor performance", *Alexandria Engineering Journal*, **51**(1), pp. 19-25 (2012).

17. Gad, H.A., AbdEl-hamid, A.A., El-Askary, W.A., et al. "A new design of Savonius wind turbine: numerical study", *CFD Letters* **6**(4), pp. 144-158 (2014).

18. Saad, A.S., El-Sharkawy. I.I., Ookawara, S., et al. "Performance enhancement of twisted-bladed Savonius vertical axis wind turbines", *Energy Conversion and Management*, **209**, 112673 (2020).

19. Layeghmand, K., Tabari, N.G., and Zarkesh, M. "Improving efficiency of Savonius wind turbine by means of an airfoil‐shaped defector", *Journal of the Brazilian Society of Mechanical Sciences and Engineering*, **42**(10), 528 (2020).

20. Yahya, W., Ziming K., Juan W., et al. "Influence of tilt angle and the number of guide vane blades towards the Savonius rotor performance", *Energy Reports*, **7**, pp. 3317-3327 (2021).

21. Mohamed, M.H., Janiga, G., Pap, E., et al. "Optimization of Savonius turbines using an obstacle shielding the returning blade", *Renewable Energy*, **35**, pp. 2618-2626 (2010).

22. Tartuferia, M., D'Alessandro, V., Montelpare, S., et al. "Enhancement of Savonius wind rotor aerodynamic performance: a computational study of new blade shapes and curtain systems", *Energy*, **79**, pp. 371-384 (2015).

23. Kalluvila, J.B.S. and Sreejith, B. "Numerical and experimental study on a modified Savonius rotor with guide blades", *International Journal of Green Energy*, **15**(12), pp. 744-757 (2018).

24. Nimvari, M.E., Fatahian, H., and Fatahian, E. "Performance improvement of a Savonius vertical axis wind turbine using a porous deflector", *Energy Conversion and Management*, **220**, 113062 (2020).

25. Hesami, A., Nikseresht, A.H., and Mohamed, M.H. "Feasibility study of twin-rotor Savonius wind turbine incorporated with a wind-lens", *Ocean Engineering*, **247**, 110654 (2022).

26. Deda Altan, B. and Gungor. A. "Enhancing the performance of Savonius wind turbines with wind router", *Iranian Journal of Science and Technology, Transactions of Mechanical Engineerin*g, (2022). Doi:10.1007/s40997-022-00580-3.

27. Tian, W., Bian, J., Yang, G., et al. "Influence of a passive upstream deflector on the performance of the Savonius wind turbine", *Energy Reports*, **8**, pp. 7488-7499 (2022).

28. Deda Altan, B. and Gungor. A. "Investigation of the turbine performances in the case of dual usage of Savonius wind turbines", *Proceedings of the Institution of Mechanical Engineers, Part E: Journal of Process Mechanical*, (2022). Doi:10.1177/09544089221140217.

29. Aboujaoude, H., Bogard, F., Beaumont, F., et al. "Aerodynamic performance enhancement of an axisymmetric deflector applied to Savonius wind turbine using novel transient 3D CFD simulation techniques", *Energies,***16**, 909, (2023). Doi:10.3390/en16020909.

30. Haddad, H.Z., Mohamed, M.H., Shabana, Y.M., et al. “Optimization of Savonius wind turbine with additional blades by surrogate model using artificial neural networks”, *Energy*, (2023). Doi: 10.1016/j.energy.2023.126952.

Biography

Burcin Deda Altan received her BSc, MSc, and PhD degrees in Mechanical Engineering from Pamukkale University, Denizli, Turkey in 1997, 2000, and 2006, respectively. She is working as an Associate Professor at the Department of Mechanical Engineering, Akdeniz University, Antalya, Turkey. Her main research interests include wind energy, other types of renewable energy, computational fluid dynamics, energy conversion and management, and fluid structure interaction.

Afsin Gungor received his PhD in Mechanical Engineering (Istanbul Technical University) in 2006. He is presently Professor of Mechanical Engineering at Akdeniz University, Antalya Turkey. Prof. Gungor has edited 15 books, has published more than 260 proceedings, and published more than 110 papers in peer-reviewed international journals, in addition to more than 30 book chapters. In the last 2 years, Prof. Gungor has applied for patents for 3 innovative projects. His research interests include new and renewable energy sources, nanotechnology, energy conversion and management, simulation and modeling of energy systems, combustion and gasification of coal and biomass in fluidized beds, hydrogen production and purification in gasification of coal and biomass, solar thermal applications.

Figure captions

Figure 1. SWT and wind collector.

Figure 2. Dimensions of the SWT.

Figure 3. Geometric dimensions of wind collector.

Figure 4. Computational domains and boundaries.

Figure 5. Stability study of the time step.

Figure 6. Time independence study of the time step.

Figure 7. Verification of the Numerical solution method.

Figure 8. A cross section from the meshed numerical study.

Figure 9. The effect of different (b/R) ratio on the coefficient of torque relative to the rotation angle of the turbine.

Figure 10. Velocity contours of various b/R ratios.

Figure 11. The effect of different (a/R) ratio on the torque-coefficient relative to the rotation angle.

Figure12. The effect of different (c/R) ratio on the torque-coefficient relative to the turbine-angle.

Figure13. The effect of different (g/R) ratio on the torque-coefficient relative to the turbine-angle.

Figure 14. The effects of geometric wind collector parameter ratios on torque coefficient.

Figure 15. Change of the power-coefficient.

Figure 16. The change of the torque-coefficient at the maximum power-coefficient.

Table captions

Table 1. Lower and upper limits of geometric ratios.

Figures

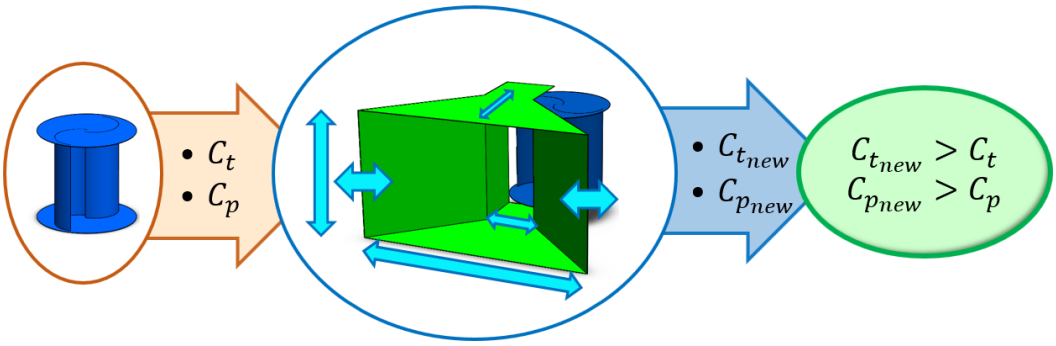

Figure 1

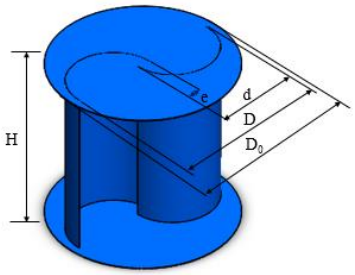

Figure 2

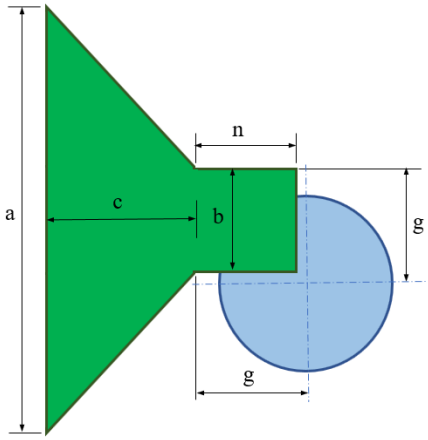

Figure 3

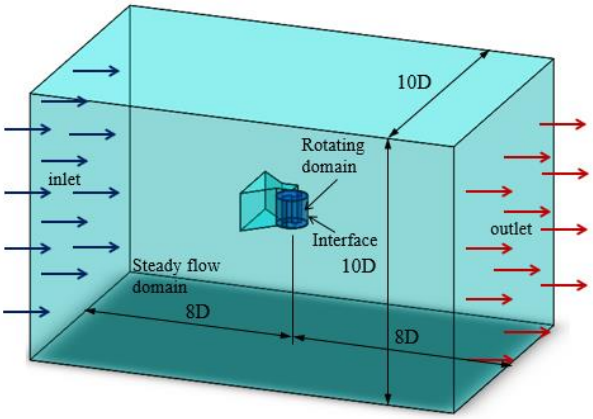

Figure 4

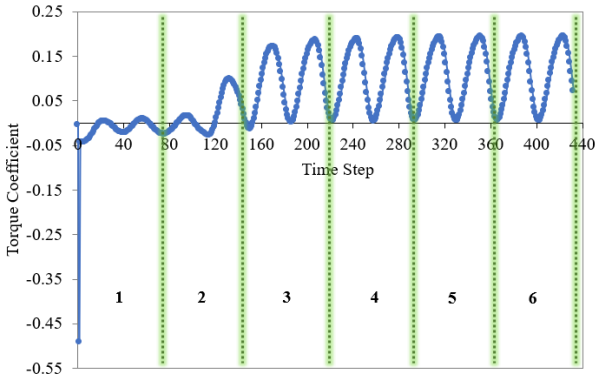

Figure 5

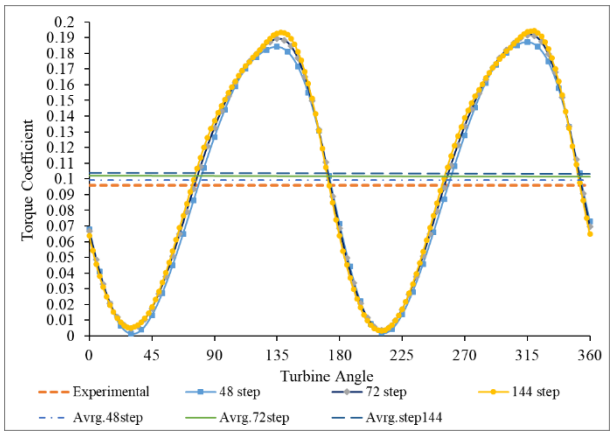

Figure 6

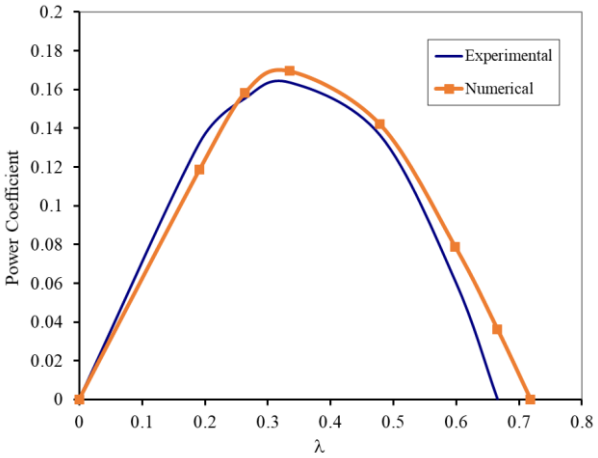

Figure 7

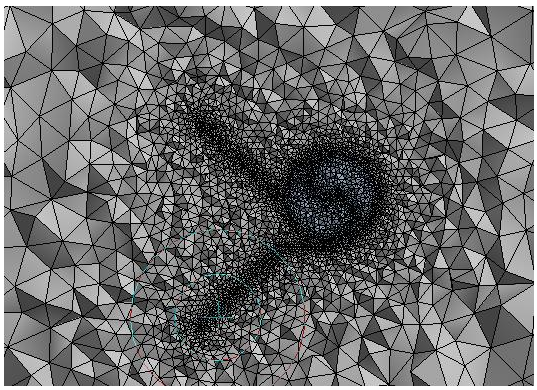

Figure 8

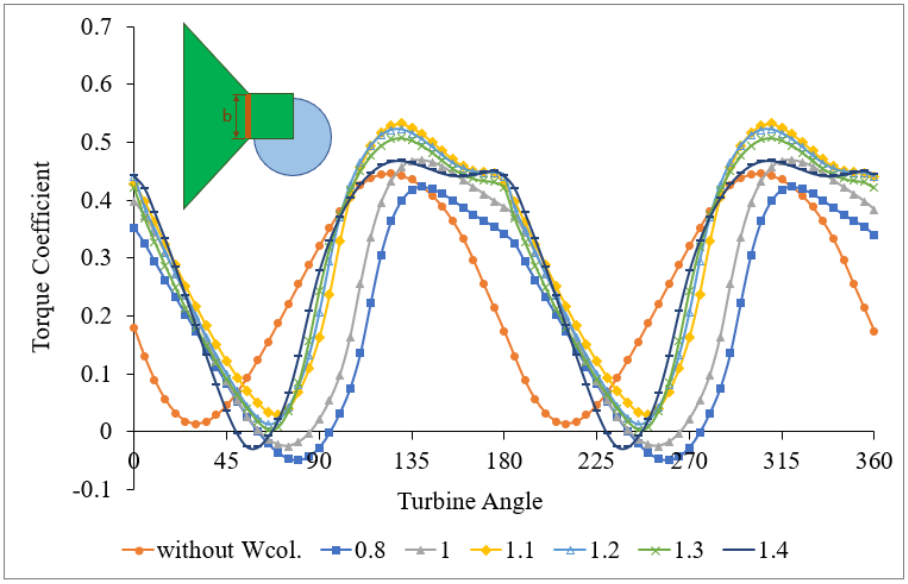

Figure 9

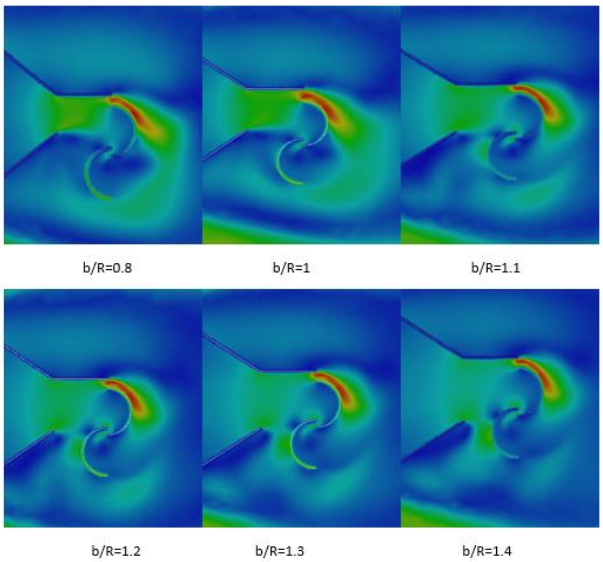

Figure 10

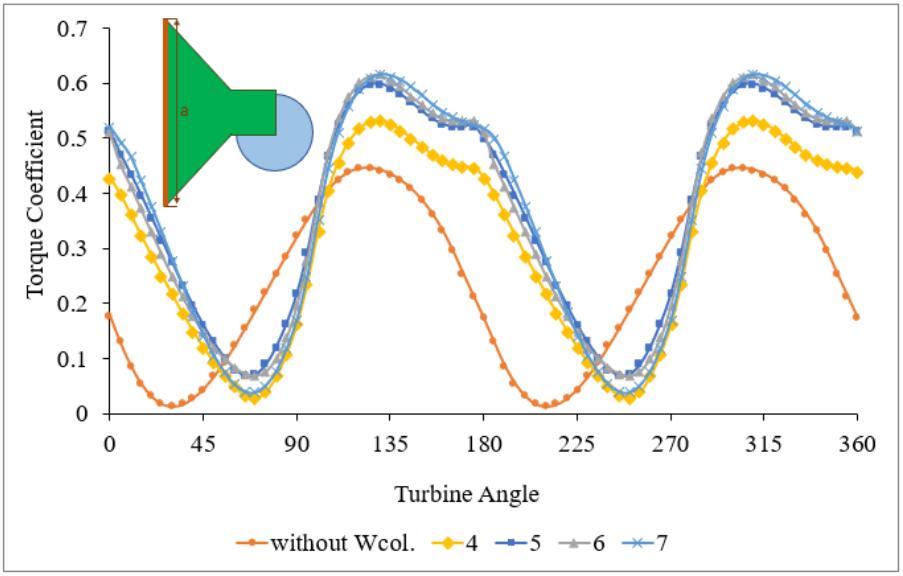

Figure 11

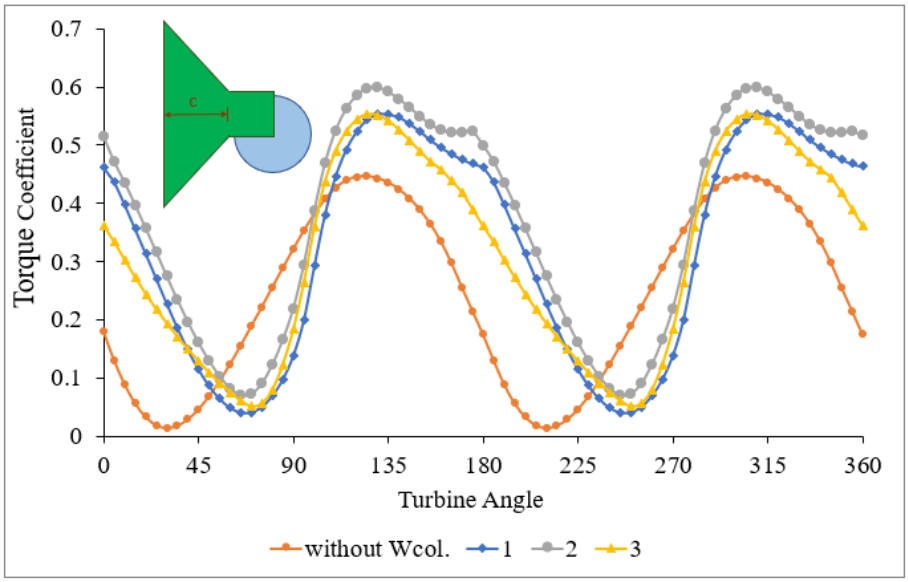

Figure12

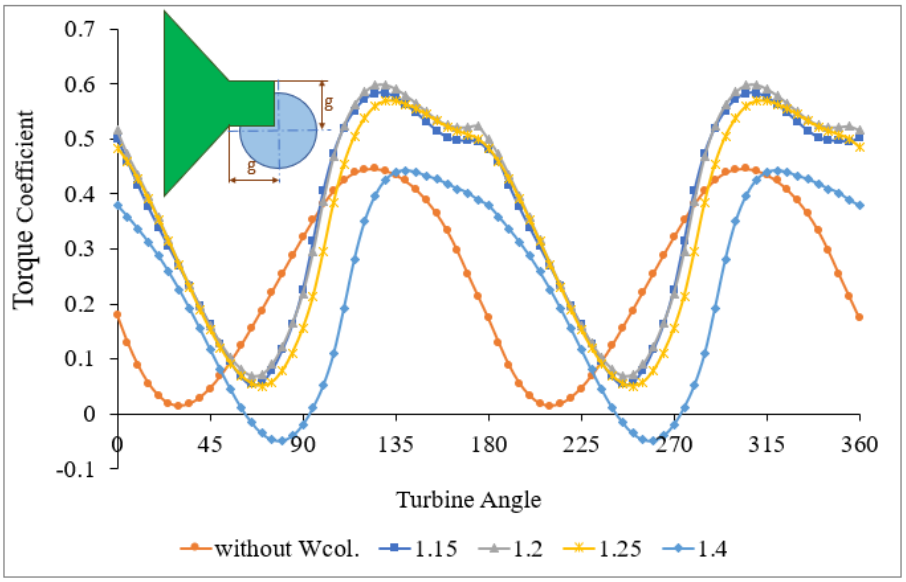

Figure13

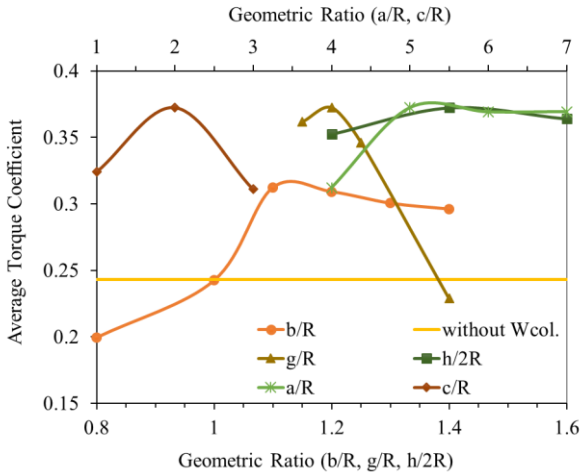

Figure 14

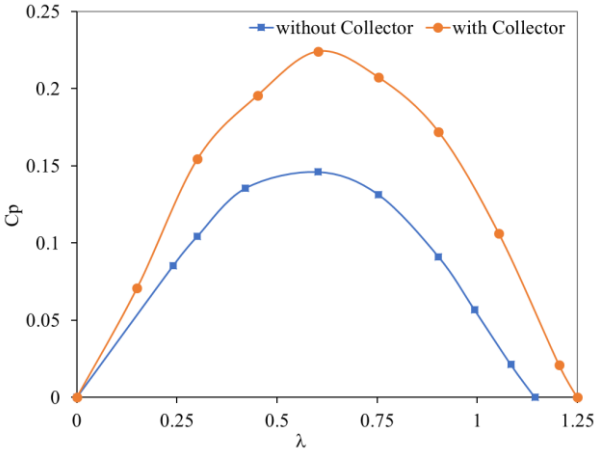

Figure 15

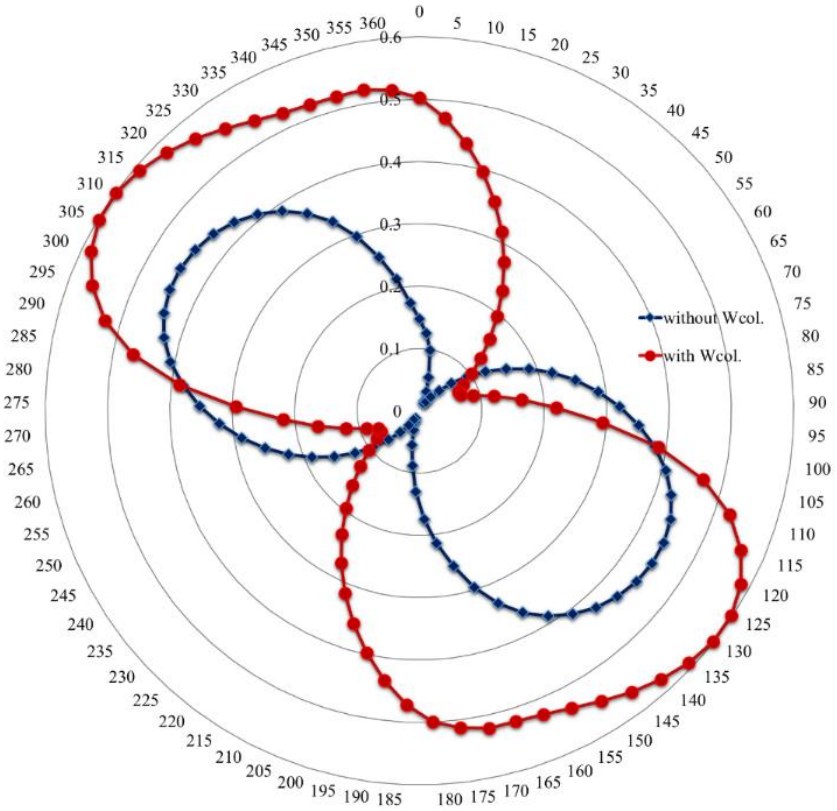

Figure 16

Tables:

Table 1

	a/R	b/R	c/R	g/R	h/2R
Lower limit	4	0.8	1	1.15	1.2
Upper limit	7	1.4	3	1.4	1.6